



THE UNIVERSITY *of* EDINBURGH

Edinburgh Research Explorer

Small influence of solar variability on climate over the past millennium

Citation for published version:

Schurer, AP, Tett, SFB & Hegerl, GC 2014, 'Small influence of solar variability on climate over the past millennium', *Nature Geoscience*, vol. 7, no. 2, pp. 104-108. <https://doi.org/10.1038/NGEO2040>

Digital Object Identifier (DOI):

[10.1038/NGEO2040](https://doi.org/10.1038/NGEO2040)

Link:

[Link to publication record in Edinburgh Research Explorer](#)

Document Version:

Peer reviewed version

Published In:

Nature Geoscience

General rights

Copyright for the publications made accessible via the Edinburgh Research Explorer is retained by the author(s) and / or other copyright owners and it is a condition of accessing these publications that users recognise and abide by the legal requirements associated with these rights.

Take down policy

The University of Edinburgh has made every reasonable effort to ensure that Edinburgh Research Explorer content complies with UK legislation. If you believe that the public display of this file breaches copyright please contact openaccess@ed.ac.uk providing details, and we will remove access to the work immediately and investigate your claim.



This is the Author's final draft or 'post-print' version following the peer review process.

Cite as: Schurer, Andrew P., Simon FB Tett, and Gabriele C. Hegerl. "Small influence of solar variability on climate over the past millennium." *Nature Geoscience* 7.2 (2014): 104-108.

DOI: 10.1038/ngeo2040

Small influence of solar variability on climate over the past millennium

Andrew P. Schurer, Simon F. B. Tett & Gabriele C. Hegerl

Address for correspondence:

Andrew Schurer
School of Geosciences,
University of Edinburgh,
Grant Institute
The King's Buildings
West Mains Road,
Edinburgh, UK
EH9 3JW
Email: a.schurer@ed.ac.uk

Small influence of solar variability on climate over the past millennium

Andrew P. Schurer¹, Simon F. B. Tett¹ and Gabriele C. Hegerl¹

¹School of Geosciences, University of Edinburgh, EH9 3JW, UK

Submitted: January 24th, 2013

Reconstructions of past climate have shown substantial decadal and centennial scale climate variability in Northern Hemisphere temperature records¹. Past studies^{2,3,4,5} have found correlations between cold temperatures and reduced solar activity during the “little ice age” and suggest a solar role in the warmth of the “Medieval Climate anomaly”. However, the amplitude of long-term changes in solar forcing is poorly constrained^{5,6}, with estimates ranging by almost an order in magnitude^{7,8,9}. Modelling studies^{10,11,12,13} indicate that a weaker solar forcing agrees better with reconstructions, but are not conclusive. Here we use model-derived fingerprints for strong and weak solar forcing as well as combinations of other forcings to determine what range of response to solar forcing is consistent with past climate. We use a methodology¹⁴ that takes into account the contribution by internal climate variability, other external drivers and uncertainty in the temperature reconstructions and in the magnitude of the model response. We find that a large solar effect on mean annual Northern Hemisphere temperatures over the past millennium is inconsistent with available temperature reconstructions, as is large solar forcing. We also find that volcanic eruptions and changes in greenhouse gases are the most important drivers of Northern Hemisphere temperature.

Estimates of the solar signal have been made from the instrumental period^{15,16} but the presence of strong anthropogenic forcings and correlations with volcanic forcing requires analysis over a long pre-anthropogenic timescale. Previous studies have considered the last millennium but were limited to Energy Balance Model fingerprints when estimating the contribution by individual forcings, and detected a solar contribution to past Northern Hemispheric and European temperature in some

reconstructions, but not in others^{17,18}. Here we make use of a targeted large ensemble of simulations with an Atmosphere-Ocean General Circulation Model HadCM3^{18,19,20} (Table 1) combined with a large ensemble of Northern Hemispheric (NH) surface air temperatures (SAT) temperature reconstructions²³ allowing us to estimate the range of contributions by solar and other external forcings that is consistent with reconstructions of the last millennium, accounting for uncertainties. The result rules out very large forcing⁷.

HadCM3 was driven with forcing estimates recommended by the third Paleoclimate Modelling Inter-comparison Project⁶ using both a weak solar forcing reconstruction^{8,9} and a very strong solar forcing⁷. Details for other forcings, such as volcanic forcing²¹, land use²², well-mixed greenhouse gases (GHGs)⁶ and orbital forcing are given in Supplementary Information. Our long simulation with all relevant forcings (**ALL long**) agrees well with the instrumental data²³ and a temperature reconstruction ensemble²⁴ (Fig. 1a), both showing warmer temperatures in the 11th and 12th centuries (the “medieval climate anomaly”) and cooler temperatures in the 17th century and early 19th century, (the “little ice age”), with pronounced recent warming. The **All long** simulation is generally within the reconstruction ensemble, with short exceptions, most notably around 1000-1100. Many of the other discrepancies are in periods immediately following volcanic eruptions, where the simulated cooling is stronger than the response in reconstructions²⁵.

Our analysis makes use of the extremely high correlation, 0.97, between the strong and weak solar forcings on inter-decadal timescales (Supplementary Fig. S2) to linearly combine the **All long** simulation with a simulation with high solar forcing; **Solar Shapiro** (where the weak solar forcing already included in **All long** is taken into account, see Supplementary Information) yielding ‘**All High Solar**’, a composite all forcing simulation with strong solar forcing. **All High Solar** is too warm during the 12th century, shows slightly lower mean correlations with the temperature reconstructions (0.51 rather than 0.54) and leaves the envelope of the reconstructions more often; 283 out of a possible 996

years compared to 141 for the **All long** run. This supports previous modelling studies which have also found poorer agreement of simulations with higher solar forcing to reconstructions^{10,11,12,13}. Importantly the high solar forcing does not help to reconcile data and models for the very earliest part of the millennium, since when reconstructed temperatures are highest, solar forcing is low¹¹.

In order to estimate the role of individual forcings, we also performed an ensemble of individually forced simulations, starting in 1400 (Fig. 1b, Table 1; also Supplementary Information), which we can use to examine the contribution each forcing makes to changes in **All long** (fig. 1b). Over the 20th century, anthropogenic forcings dominates with GHGs the largest forcing, offset by the effect of anthropogenic aerosols and land use changes (Fig. 1c). Simulated pre-industrial changes in NH temperature are substantial but much smaller than the 20th century increase. Volcanic aerosols not only lead to sharp transient drops in hemispheric temperatures but are also responsible for cooler climate over longer time scales^{10,11,17,20}. For example the large volcanic cooling seen in 1790-1830 (Fig. 1c, Supplementary Fig. S5). Fluctuations in the concentration of GHGs also have an impact, even before the simulated anthropogenic increase becomes apparent by the mid-19th century with a GHG induced cooling during the 17th century (Supplementary, Fig. S4).

The weak solar forcing is the smallest forcing we consider within the model (Figs. 1b,c), and does not show a significant effect on NH mean temperature during the three solar minima highlighted in Fig. 1c. The strong solar forcing gives 0.3K and 0.4K simulated cooling for the Maunder (1645-1715) and the Spörer (1460-1550) minima respectively. In the large solar forcing scenario the strongest pre-industrial forcing is solar.

In order to resolve if solar forcing is a large or small contributor to NH mean temperatures, we estimate the magnitude of the response to solar and other forcings directly from temperature reconstructions. We do this by deriving a decadal smoothed (see Supplementary Information) “fingerprint” of expected

change for NH SAT from each model ensemble that is driven by a particular external forcing (e.g. solar). The magnitude of this fingerprint is then estimated for each reconstruction, accounting for uncertainty both in the magnitude of the forcing and the sensitivity to forcing. This is done by ‘scaling factors’ that are determined by minimizing the difference between the reconstruction and a linear combination of fingerprints, using total least squares regression¹⁴ (see methods). Therefore, we do not need to explicitly investigate different forcing amplitudes.

We consider several important sources of uncertainty (see methods). Uncertainty in reconstruction method and proxy choice is estimated using the Frank et al.²⁴ ensemble of 521 annual NH (0-90N, land and ocean) SAT reconstructions. This ensemble was derived from 9 independent published reconstructions each using a different reconstruction technique and different proxy sources. However, that many local records are shared between reconstructions). Uncertainty arising from the choice of calibration period is sampled within the reconstruction ensemble²⁴. Uncertainty arising from the presence of internal climate variability in both fingerprints and reconstructions is estimated using variability taken from the control simulations of four different climate models. We only use regression results for which the residual variability is consistent with the model derived estimates of internal variability (see methods and Supplementary Information). However our key results are insensitive to this criterion (Supplementary Fig. S11).

We first carried out the analysis for 1000-1900; deriving fingerprints for all forcings and solar forcing from the NH SAT **All long** and **Solar Shapiro** simulations. The results of the multiple regression can be interpreted to estimate the linear scaling (Fig. 2a) for solar forcing and for all forcings other than solar forcing (termed **ALL_nosol**, see methods). Approximately 90% of the reconstructions have residuals consistent with model internal variability (Supplementary Table S2). For these consistent reconstructions we detected the effect of **ALL_nosol** in all the reconstructions, indicating a clear response of NH SAT to external forcing. The estimated amplitude of the solar response is consistent

with both no, or a weak solar forcing response. None of the scaling values found supports an estimated solar response as large as the simulated response to the Shapiro forcing.

We determined the role of individual forcings using fingerprints for 1451-1900 from our individually forced simulations, a period when temperature reconstructions are based on more and denser sampled data, thus providing a better constraint¹. The contribution from volcanic, solar and GHG forcings can be estimated separately using fingerprints of NH SAT taken from the **VOLC**, **GHG** and **Solar Shapiro** simulations. Other forcings have a small *simulated* impact during this period (Fig. 1). We find a detectable volcanic signal in all reconstructions, indicating the clear presence of a volcanic effect (Figs. 2b,d). The majority of scaling factors are less than one, which indicates that the forced response to volcanic eruptions is likely larger in the simulations than in the reconstructions. This could be due to errors in the forcing, an overestimate of the forcing by large eruptions²⁶, a muted response in proxy records^{27,28}, a too strong model response, or a combination of these²⁵. The GHG fingerprint was detected in 85% of reconstructions as well as in the average reconstruction, indicating a detectable role of GHGs prior to 1900 (Figs. 2c,d). Since the 5-95% range for β encompasses unity the results are consistent with a correctly modelled response to this forcing. The 5-95% range of the solar forcing is again compatible both with no or a weak effect from solar forcing, but rules out a role of solar response as large as that in **Solar Shapiro** (Fig. 2b,c). The scaling factors for the solar and volcanic fingerprint are quite well separated, indicating that the solar and volcanic response can be well separated from inter-decadal data, despite correlation, on long timescales (Fig. 2b and supplementary Fig. S6). The confidence intervals estimated for the average reconstruction, which arise entirely from internal variability, are much smaller than the confidence interval from the combined results from individual reconstructions. This indicates that a large part of the uncertainty in the estimated contribution by forcings arises from differences between reconstructions.

These results can be used to estimate the contribution to actual reconstructed inter-decadal NH

temperature variability by individual forcing (Fig. 2e). Volcanic and GHG forcings appear to contribute most to pre-20th climate variability, while the contribution by solar forcing is modest, agreeing with the simulations with low solar forcing. The 95% upper limit on the solar scaling factor β rules out a solar contribution since the Maunder Minimum that is greater than about 0.15K. Although solar forcing may be relatively unimportant for large-scale climate change, it could still play a significant role in regional and seasonal variability^{5,29} due to its influence on climate dynamics, an influence that is strongly diminished when averaging annually and over the whole NH. Similarly, missing solar-ozone feedback in our model³⁰ should also predominantly impact regional temperatures⁵. Should it, however, enhance the NH temperature response to solar forcing it would result in smaller (not larger) scaling factors (Fig. 2).

We believe that our results are robust despite remaining uncertainties. Though our fingerprints are taken from simulations with a single climate model our results depend on only the temporal pattern of the fingerprint time series and not on its magnitude, as an incorrect magnitude would be corrected by the scaling factor. Smoothed hemispheric mean timeseries using different models driven with combined forcings are highly correlated, suggesting that our results are largely model independent (Supplementary Fig. S7). A perfect model analysis shows that we can retrieve the response to known large solar forcing from a simulation with a different climate model (Supplementary Fig. S8). In contrast, and similar to results based on reconstructions, the solar forcing fingerprint is not detectible in simulations with weak solar forcing. Furthermore, our method does not allow for nonlinearities in combinations of forcings, but such effects are small in HadCM3 (Supplementary Fig. S9).

Though our results rule out solar forcing as a strong driver of pre-20th century NH temperature variability this does not, in itself, rule out the possibility of strong solar forcing. However, for solar forcing to be large the response to it would have to be almost an order of magnitude smaller in the real world than in the model, with the sensitivity to it dramatically different from the sensitivity to other

forcings (Fig. 2). As we consider this highly unlikely, we conclude that large solar forcing is inconsistent with reconstructions of climate of the past millennium.

Methods:

To estimate the contribution of combinations of different forcing to NH SATs we use **total least squares (TLS)**¹⁴ regression which allows for the presence of noise in the regressor and regressor target.

$$Y(t) = \sum_{i=1}^m (X_i(t) - v_i(t))\beta_i + v_0(t) . \quad (1)$$

This assumes that the temperature reconstruction, Y , is a linear combination of m different fingerprints X_i for the response to different external forcing, taken from simulations. Each fingerprint has associated internal variability v_i (with variance that is reduced due to ensemble averaging), and the reconstruction contains a realization of internal variability v_0 . The scaling factors β_i determines the magnitude of the fingerprint in reconstructions, and the response to a forcing is considered detectable if its scaling factor is significantly positive. For both the model fingerprints and control simulations spatial annual means of 0-90N land and sea are calculated corresponding to the area represented by the reconstructions. All reconstructions and model simulations are decadal smoothed (see SI). The scaling factors β_i and the noise-reduced fingerprints and reconstructions, \tilde{Z} (i.e. an estimate of the true underlying response to forcing as represented in model simulations \tilde{X} , and reconstructions, \tilde{Y}) are calculated following Allen and Stott¹⁴, where:

$$\begin{aligned} \tilde{Z} &= [\tilde{Y}, \tilde{X}] \\ \tilde{Y} &= Y(t) - v_0(t) \quad \tilde{X} = \sum_{i=1}^m (X_i(t) - v_i(t)) \end{aligned} \quad (2)$$

To evaluate the self-consistency of the regression result the residuals were checked against estimates of

model-based internal variability. If a fit to a reconstruction yields a regression residual with a chi-squared value (eq. 26 in Allen and Stott¹⁴) that is smaller than the sum-of-squares of ~90% of the control samples it is included in further analysis, if not, the results for that reconstruction are not used as the regression residual is not consistent with the assumption made in eq. 1, (this is the same test as is used in ref. 24). To construct the model based samples of internal variability used for this test, we use control simulations from 4 different model simulations (HadCM3, GISS-E2-R, MPI-COMOS and MPI-ESM-P, for details see SI section 5) which are sliced into 14 and 18 non-overlapping chunks for use with the analysis periods 1000-1900 and 1401-1900 respectively. For the former, the fit is rejected if the residual is larger than 2 of the 14 samples, in the latter case it is rejected if larger than 3 of the 18 samples. The uncertainty due to internal variability is then calculated by superimposing different random samples of the model-based internal variability onto both noise reduced observations and model fingerprints \tilde{Z} . This is repeated 2000 times to calculate a distribution of 2000 β -values.

The 2000 realisations of β for all reconstructions which pass the consistency test are then combined together to form one distribution. This distribution accounts for uncertainty in both reconstruction and internal variability. The 5-95% range and median value of β are then calculated from this distribution. The analysis is also repeated using the mean of all 521 reconstructions.

For 1000-1900, a multiple linear regression of the reconstructions on **All long** and **Solar Shapiro** fingerprints was performed:

$$Y = \beta_1(\text{ALL long} + v_1) + \beta_2(\text{Solar Shapiro} + v_2) + v_0 \quad (3)$$

$$Y = \beta_1\left(\frac{\text{Solar Shapiro}}{\alpha} + \text{ALL nosol} + v_1\right) + \beta_2(\text{Solar Shapiro} + v_2) + v_0 \quad (4)$$

This makes use of **All long** containing a contribution from the weak solar forcing, assuming that **All long** is a sum of the effect of solar forcing and an effect from all other forcings (All_nosol), and that the

strong forcing is, for the filtered data, a scaled version of the weak forcing (see SI). Rearranging this for All_nosol and Solar_shapiro separately yields scaling factors for those forcings:

$$\beta_{\text{All_nosol}} = \beta_1 \quad (5)$$

$$\beta_{\text{Solar (Shapiro)}} = \frac{\beta_1}{\alpha} + \beta_2 \quad (6)$$

Where $\alpha = 8.5$ (see SI).

For the 1400-1900 period the **Solar Shapiro** simulation, the ensemble mean of the **GHG** simulations and the ensemble mean of the **VOLC** simulations were used as externally forced fingerprints (X_i) for a three fingerprint analysis (i.e. m is equal to 3 in eq. 1). The **Solar Shapiro** simulation was used instead of the ensemble mean of **Weak Solar** because the signal-to noise ratio of the **Weak Solar** simulations was too low to be detectable (see SI, fig S8c).

To derive the contribution to inter-decadal NH temperature variability by the individual forcings the noise reduced fingerprints \tilde{X} , calculated through the TLS analysis, for each fit which passed the consistency test, were scaled by their best estimate β values and the standard deviation calculated. The median and 5-95% range was then calculated from the distribution. The standard deviation of internal variability was calculated for each TLS fit which passed the residual consistency test. It was taken as the maximum standard deviation of any of the samples of internal variability $v_{0..n}$ in eq. 1, calculated from the difference between the original observations and fingerprints, and their noise-reduced counterparts, \tilde{Z} . The median value and 5-95% range was taken from the resulting distribution.

Correspondence and requests for material should be directed to Andrew Schurer, email:

a.schurer@ed.ac.uk

Acknowledgements: Work funded by NERC grant NE/G019819/1. We acknowledge CMIP5 and

PMIP3, and we thank the climate modelling groups (listed in section 6 of the SI) for producing and making available their model output, Gareth Jones for making a long HadCM3 control simulation available for our use, David Frank for making his reconstructions available, for providing code to perform the cubic spine smoothing and for several helpful comments and Matthew Williams, Julia Pongratz and Thomas Crowley for advice in forcing implementation.

Author Contributions: AS & ST set up and carried out the simulations. AS & GH carried out the fingerprinting analysis. All contributed to the writing and the design of modelling and analysis strategy.

References:

1. Jansen, E. *et al.* in *IPCC Climate Change 2007: The Physical Science Basis* (eds Solomon, S. *et al.*) 433–497 (Cambridge Univ. Press, 2007).
2. Eddy, J.A. Maunder Minimum. *Science*, **192**, 1189–1202 (1976)
3. Swingedouw, D., L. Terray, C. Cassou, A. Voldoire, D. Salas-Mélia, and J. Servonnat. Natural forcing of climate during the last millennium: Fingerprint of solar variability. *Clim. Dyn.* **36**, 1349–1364 (2011).
4. Van Hateren J. H. A fractal climate response function can simulate global average temperature trends of the modern era and the past millennium *Clim. Dyn.* **40**, 2651–2670 (2012)
5. Gray, L. J. *et al.* Solar influences on climate. *Rev. Geophys.* **48**, RG4001 (2010).
6. Schmidt, G. A. *et al.* Climate forcing reconstructions for use in PMIP simulations of the last millennium (v1.1). *Geosci. Model Dev.* **5**, 185–191 (2012)
7. Shapiro, A. I., *et al.* A new approach to the long-term reconstruction of the solar irradiance leads to large historical solar forcing. *Astron. & Astrophys.*, **529**, A67 (2011).
8. Steinhilber, F., Beer, J., and Fröhlich, C. Total solar irradiance during the Holocene, *Geophys. Res. Lett.*, **36**, L19704 (2009).
9. Wang, Y.-M., Lean, J. L., & Sheeley, N. R. Modeling the Sun’s magnetic field and irradiance since

1713. *The Astrophys. J.* **625**, 522–538 (2005).
10. Ammann, C. et al. Solar influence on climate during the past millennium: Results from transient simulations with the NCAR Climate System Model. *Proc. Natl Acad. Sci. USA* **104**, 3713-3718 (2007).
 11. Jungclauss, J. H., et al. Climate and carbon-cycle variability over the last Millennium. *Clim. Past Discuss.* **6**, 1009-1044, (2010).
 12. Feulner G. Are the most recent estimates for Maunder Minimum solar irradiance in agreement with temperature reconstructions? *Geophys. Res. Lett.* **38**:L16706 (2011).
 13. Hind A, & Moberg A. Past millennial solar forcing magnitude. *Clim. Dyn.* Online First (2012)
 14. Allen, M. R. & Stott, P. A. Estimating signal amplitudes in optimal fingerprinting, Part I: Theory. *Clim. Dyn.* **21**, 477-491 (2003).
 15. Stott, P. A., Jones, G. S. & Mitchell, J. F. B. Do models underestimate the solar contribution to recent climate change? *J. Clim.* **16**, 4079–4093 (2003)
 16. Benestad, R.E. & Schmidt, G.A. Solar trends and global warming *J. Geophys. Res.* **114**, (2009)
 17. Hegerl, G. C. *et al.* Detection of human influence on a new 1500 yr climate reconstruction. *J. Clim.* **20**, 650-666 (2007).
 18. Pope, V. D. Gallani, M. L. Rowntree, P. R. and Stratton, R. A. The impact of new physical parametrizations in the Hadley Centre climate model - HadAM3. *Clim. Dyn.*, **16**, 123-146 (2000).
 19. Gordon, C. *et al.* The simulation of SST, sea ice extents and ocean heat transports in a version of the Hadley Centre coupled model without flux adjustments. *Clim. Dyn.*, **16**, 147-168 (2000)
 20. Tett, S. F. B. et al. The impact of natural and anthropogenic forcings on climate and hydrology since 1550. *Clim. Dyn.* **28**, 3-34 (2007).
 21. Crowley, T. J. et al. Volcanism and the little ice age. *PAGES News* **16**, 22-23 (2008).
 22. Pongratz, J. Reick, C. Raddatz, T. and Claussen M. A reconstruction of global agricultural areas and land cover for the last millennium. *Global Biogeochem. Cycles* **22**, GB3018, (2008)
 23. Morice, C. P. Kennedy, J. J. Rayner, N. A. and Jones, P. D. Quantifying uncertainties in global and

regional temperature change using an ensemble of observational estimates: The HadCRUT4 data set. *J. Geophys. Res.* **117**, D0810 (2012)

24. Frank, D. C. *et al.* Ensemble reconstruction constraints on the global carbon cycle sensitivity to climate. *Nature* **463**, 527-530 (2010).
 25. Schurer, A. P. Hegerl, G. C. Mann, M. E. Tett, S. F. B. Phipps, S. J. Separating Forced from Chaotic Climate Variability over the Past Millennium. *J. Climate*, **26**, 6954–6973 (2013).
 26. Timmreck, C. *et al.* Limited temperature response to the very large AD 1258 volcanic eruption. *Geophys. Res. Lett.* **36**, L21708 (2009)
 27. Mann, M. E. Fuentes, J. D. and Rutherford, S. Underestimation of volcanic cooling in tree-ring-based reconstructions of hemispheric temperatures. *Nat. Geosci.* **5**, 202–205 (2012)
 28. Anchukaitis, K. *et al.* Tree rings and volcanic cooling. *Nat. Geosci.*, **5**, 836–837 (2012)
 29. Woollings, T., Lockwood, M. Masato, G. Bell, C. and Gray, L. Enhanced signature of solar variability in Eurasian winter climate. *Geophys. Res. Lett.* **37**, L20805 (2010).
 30. Shindell, D. T. Faluvegi, G. Miller, R. L. Schmidt, G. A. Hansen, J. E. and Sun, S. Solar and anthropogenic forcing of tropical hydrology. *Geophys. Res. Lett.*, **33**, L24706 (2006)
- Hegerl, G., *et al.* Influence of human and natural forcing on European seasonal temperatures. *Nature Geoscience*. **4**, 2, 99-103 5 (2011)

<i>Name</i>	<i>Years (C.E.)</i>	<i>No. of runs</i>	<i>Forcings</i>						
			<i>Solar</i>	<i>Volcs</i>	<i>GHGs</i>	<i>LUSE</i>	<i>AER</i>	<i>O₃</i>	<i>Orb</i>
<i>All long</i>	800- 2000	1	✓	✓	✓	✓	>1820	✓	✓
<i>CTL850</i>	800- 2000	1	850	800- 850	800- 850	825	0	PI	825
<i>Solar Shapiro</i>	800- 2000	1	✓ Shapiro	800- 850	800- 850	825	0	PI	825
<i>All</i>	1400- 2000	3	✓	✓	✓	✓	>1820	✓	✓
<i>Weak Solar</i>	1400- 2000	4	✓	0	1400	1400	0	PI	1400
<i>VOLC</i>	1400- 2000	3	1400	✓	1400	1400	0	PI	1400
<i>GHG</i>	1400- 2000	4	1400	0	✓	1400	0	PI	1400
<i>NoLUSE</i>	1400- 2000	4	✓	✓	✓	1400	>1820	✓	✓
<i>NoAER</i>	1750- 2000	4	✓	✓	✓	✓	0	✓	✓

Table 1 - Details of experimental design. A tick indicates where the simulations included the forcing for the whole time period. **AER** indicates aerosols and **LUSE** Land use. Where a single year or range is given the forcing was constant at the year or range. **PI** is pre-industrial ozone.

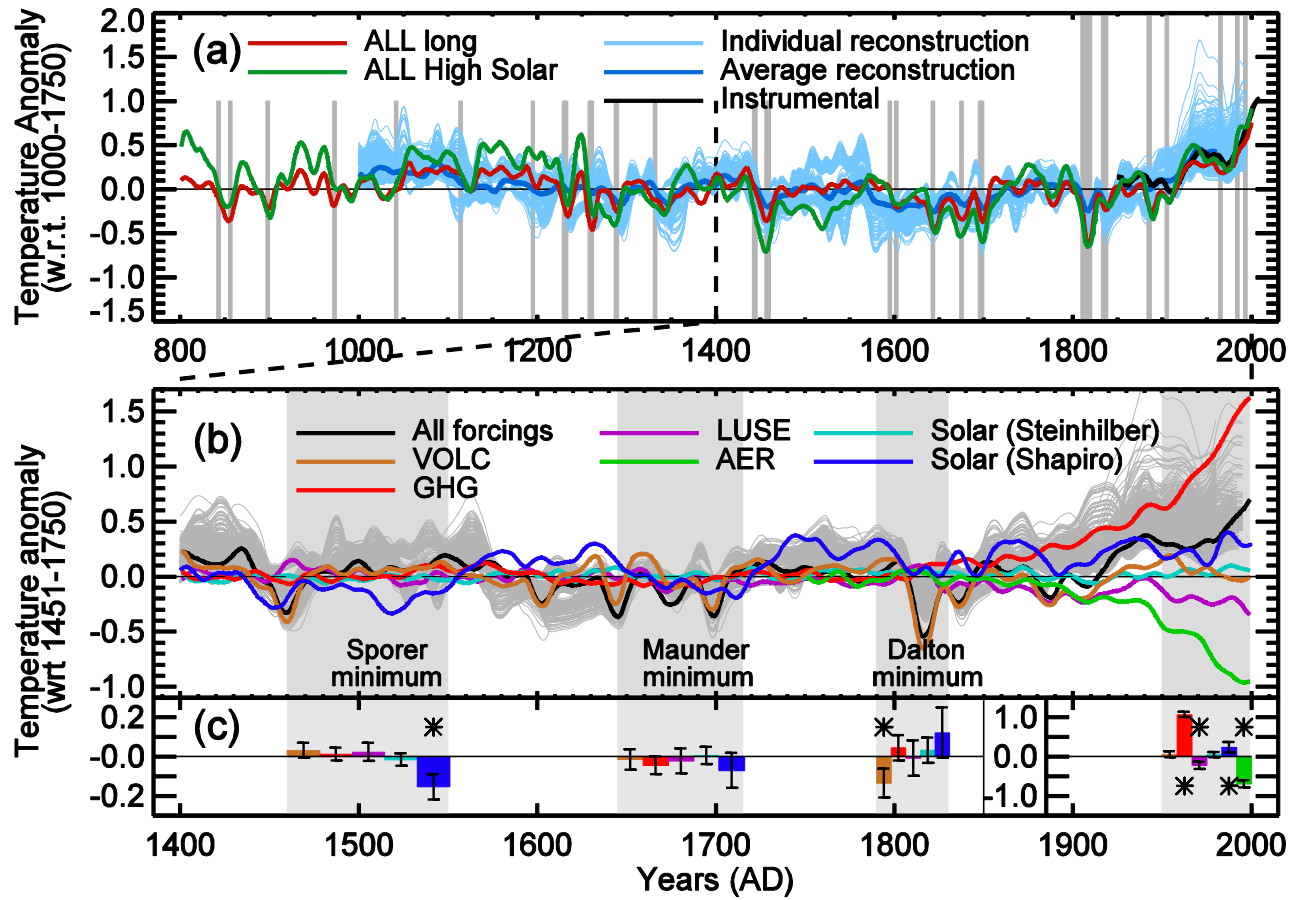


Fig. 1: Simulations and temperature reconstructions. (a) Simulations with all forcings (coloured) compared to a reconstruction ensemble (blue)¹⁴, and instrumental HadCRUT4³⁰ time series (centred on the average reconstruction over time of overlap, black). Major volcanic eruptions are shown as grey vertical lines. (b) Ensemble mean individual forcing experiments (colour, see Table 1) compared to reconstruction ensemble (light grey). (c) Simulated contribution by individual forcings (colours as in b) to periods coinciding with three solar minima (highlighted grey in b) and the last 50-years (note different scale) with their 95% uncertainty. An asterisk indicates when the contribution by a forcing is significant at the 5% level (see Supplementary Information).

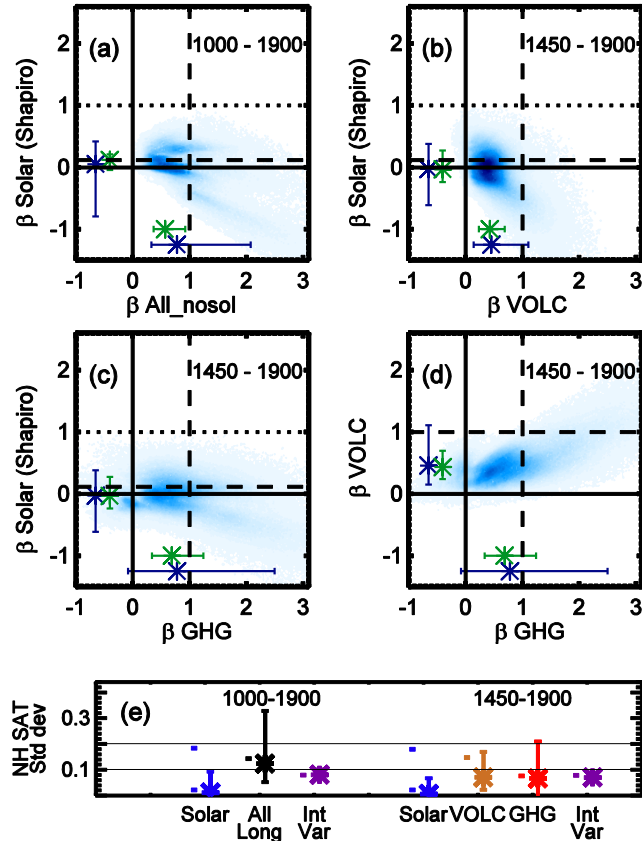


Fig. 2: Estimated response to forcings (a) Amplitude of *ALL_nosol* (horizontal) and *Solar Shapiro* (vertical) for 1000-1900. (b,c,d) Amplitudes of *VOLC*, *GHG* and *Solar Shapiro* for 1450-1900. In plots a-d blue shading shows joint probability density of β values (see methods). Vertical and horizontal lines show β for a signal that is absent from the reconstructions (solid), consistent with the forcing in *All long* (dashed), and consistent with strong solar forcing⁷ (dotted). Bars show the 5-95% range of individual signal amplitudes using all reconstructions (blue) and the average reconstruction (green). (e) Estimated contribution by forcings to NH inter-decadal variability (one standard-deviation). Cross shows best estimate, bar the 5-95% range, and short dash to the left the un-scaled model results with both the low and high solar forcings.